Crossing Over from Attractive to Repulsive Interactions in a Tunneling Bosonic Josephson Junction

Crossing Over from Attractive to Repulsive Interactions in a Tunneling Bosonic Josephson Junction

G. Spagnolli,[1] G. Semeghini,[1] L. Masi,[2] G. Ferioli,[2] A. Trenkwalder,[1] S. Coop,[2,3] M. Landini,[1] L. Pezzè,[4,1,2] G. Modugno,[2] M. Inguscio,[2,1] A. Smerzi,[4,1,2] and M. Fattori[2,1]

[1]*CNR Istituto Nazionale Ottica, 50019 Sesto Fiorentino, Italy*

[2]*LENS and Dipartimento di Fisica e Astronomia, Universitá di Firenze, 50019 Sesto Fiorentino, Italy*

[3]*ICFO-Institut de Ciencies Fotoniques, Barcelona Institute of Science and Technology, 08860 Castelldefels (Barcelona), Spain*

[4]*Quantum Science and Technology in Arcetri, QSTAR, 50125 Firenze, Italy*

(Received 30 September 2016; published 9 June 2017)

We explore the interplay between tunneling and interatomic interactions in the dynamics of a bosonic Josephson junction. We tune the scattering length of an atomic ^{39}K Bose-Einstein condensate confined in a double-well trap to investigate regimes inaccessible to other superconducting or superfluid systems. In the limit of small-amplitude oscillations, we study the transition from Rabi to plasma oscillations by crossing over from attractive to repulsive interatomic interactions. We observe a critical slowing down in the oscillation frequency by increasing the strength of an attractive interaction up to the point of a quantum phase transition. With sufficiently large initial oscillation amplitude and repulsive interactions, the system enters the macroscopic quantum self-trapping regime, where we observe coherent undamped oscillations with a self-sustained average imbalance of the relative well population. The exquisite agreement between theory and experiments enables the observation of a broad range of many body coherent dynamical regimes driven by tunable tunneling energy, interactions and external forces, with applications spanning from atomtronics to quantum metrology.

DOI: 10.1103/PhysRevLett.118.230403

Introduction.—The Josephson junction is a paradigmatic device for the observation of coherent quantum phenomena on meso- or macroscopic scales with technological applications in precision measurements and sensing [1]. Traditional junctions consist of two superconducting bulks separated by a thin insulator [2] or two superfluid helium baths coupled through nanoapertures [3,4]. Nonlinearities in weakly coupled Bose-Einstein condensates (BECs) further enrich the Josephson physics with novel phenomena, such as bifurcations, anharmonic population or phase oscillations, and macroscopic quantum self-trapping (MQST) [5]. Bosonic Josephson junctions have been extensively studied theoretically [5–7] and different experiments have demonstrated coherent tunneling oscillations of interacting bosons [8], Josephson plasma oscillations [9–12], the analog of the dc and ac regimes [13], and self-trapping [9]. Nonlinear Josephson dynamics in the presence of strong dissipation have been investigated with cavity polaritons [14,15].

However, all Josephson junctions experimentally investigated so far have been realized with a strong repulsive interaction (positive "charging" energy) among the superfluid or superconducting particles. Josephson junctions with negative charging energy, i.e., attractive interparticle interactions, are predicted to manifest a critical slowing down of the small-amplitude oscillations. Furthermore, with weak repulsive interactions, the frequencies are expected to deviate from the plasma scaling while crossing over from the Josephson to the noninteracting Rabi regime, a scenario that has not been experimentally accessible so far.

In this Letter, we study the tunneling dynamics of an atomic BEC with tunable interactions in a double-well potential. By exploiting a magnetic Feshbach resonance [16], the scattering length a_s is changed from positive to negative, while crossing over the limit of noninteracting atoms. With zero interatomic interactions, $a_s = 0$, we observe Rabi oscillations of the atomic cloud between the two separated spatial modes. By increasing the strength of the repulsive interaction, $a_s > 0$, we investigate the interplay between Rabi and Josephson plasma oscillations up to the point where, for larger initial population imbalances, the system enters the MQST regime. MQST is characterized by high-frequency coherent population oscillations driven by a monotonically increasing phase. In contrast, an increasingly negative scattering length, $a_s < 0$, corresponding to an attractive interatomic interaction, slows down the dynamics of the system until the plasma oscillation vanishes. This corresponds to the critical point of a parity-symmetry breaking quantum phase transition [17]. Our studies provide the benchmark characterization of a bosonic Josephson junction in dynamical regimes not attainable with other superconducting or superfluid systems. The tunable interaction paves the way for the observation of several many-body phenomena [18–20] and for the realization of spatial interferometry devices (built with the two spatial modes of the double-well potential) with quantum enhanced sensitivity [21–23]. Indeed, the possibility of tuning the interaction in the double-well BEC will allow us to exploit large

nonlinearities for the preparation of many-body quantum-entangled states [24] and to cancel the scattering length during the interferometer operations. This will enable the realization of a spatial linear Mach-Zehnder interferometer with sub-shot-noise phase resolution.

Our experimental setup is similar to that used in a previous work [17,25]. We create atomic ^{39}K BECs in the $F = 1$, $mF = 1$ state with tunable interactions by exploiting a magnetic Feshbach resonance centered around 400 Gauss [26]. The BEC, with an atom number N between 2000 and 8000, is trapped in a double-well potential made by a single periodic unit of an optical superlattice, i.e., two superimposed optical lattices with a periodicity of $\lambda_p/2 = 10\ \mu$m (primary lattice) and $\lambda_s/2 = 5\ \mu$m (secondary lattice), respectively. The primary lattice has a depth of $k_B 40$ nK, where k_B is the Boltzmann constant, and by changing the intensity of the secondary lattice, we can adjust the height of the barrier between the two wells. The position of the barrier is controlled by the relative frequency of the two lattice lasers. This allows us to control the finite energy difference between the two wells and (in the experiments discussed below) to load the atomic cloud with an initial population imbalance. For experiments, we start from an imbalanced cloud and center the barrier within $\approx$10 ms, bringing the cloud out of equilibrium. Then, we observe the system evolution as a function of time, measuring both the population imbalance and the relative phase between the BECs in the two wells [25].

Rabi oscillations.—We create a BEC made of noninteracting atoms by tuning the scattering length to $a_s = 0$ and measuring the oscillations of the population imbalance between the two wells of the potential, see Fig. 1. In this limit, the BEC dynamics is governed by the Schrödinger equation $i\hbar\dot{\Psi} = H_0\Psi$, where $H_0 = -\hbar^2\nabla^2/2m + V(\boldsymbol{r})$ and m is the mass of the potassium atom. Here, $V(\boldsymbol{r}) = V_{\rm dw}(x) + \frac{1}{2}m\omega_\perp^2 r_\perp^2$ is the trapping potential, given by a radial harmonic trap of frequency $\omega_\perp = 2\pi \times 200$ Hz, and a double-well (dw) potential $V_{\rm dw}(x)$ along the x axis. The lowest energy longitudinal excitations can be described in terms of two modes, $\Psi(\boldsymbol{r}, t) = c_L(t)\psi_L(\boldsymbol{r}) + c_R(t)\psi_R(\boldsymbol{r})$, where $\psi_L = (\psi_g + \psi_e)/\sqrt{2}$ and $\psi_R = (\psi_g - \psi_e)/\sqrt{2}$ are a linear superposition of the single particle symmetric ground state ψ_g and the antisymmetric (along the x direction) first excited state ψ_e. For high enough tunneling barriers, the two complex amplitudes $c_{\rm L,R}(t)$ of the superposition are related to the macroscopic observables of the junction, i.e., the conjugate atomic imbalance $z = (N_L - N_R)/N = |c_L|^2 - |c_R|^2$ and the relative phase $\phi = \arg(c_L) - \arg(c_R)$. Oscillations occur at a Rabi frequency $\omega_R = (E_e - E_g)/\hbar = 2K_s/\hbar$, where $K_s = \int d^3\boldsymbol{r}\psi_R H_0 \psi_L$ is the tunneling energy. Changing the barrier height allows the control of the oscillation frequency from values that are comparable to the trapping frequency in a single site of the primary lattice $\omega_x \approx 2\pi \times 150$ Hz to sub-Hz values. Direct measurements of the Rabi oscillations are possible down to a few Hz where residual instabilities of the energy difference between the two wells become non-negligible. As expected from the linearity of the system, the oscillation frequencies are independent of the initial imbalance (see Fig. 1). We can drive oscillations around $z = 0$ not only with an initial phase $\phi = 0$, but also, with $\phi = \pi$, see [25]. Note that, although linear coupling between internal states is a well established technique in atomic, molecular, and optical physics, this is the first time that a linear coupling between two trapped spatial modes occupied by an atomic BEC is demonstrated.

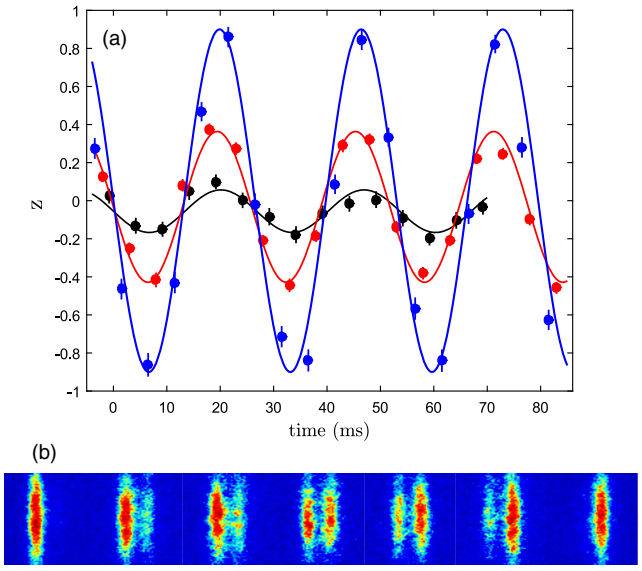

FIG. 1. Observation of Rabi oscillations. (a) Atomic imbalance z evolution for $a_s = 0$ and for three different oscillation amplitudes. Lines are sinusoidal fits to the data. (b) Absorption images of the BEC during half oscillation.

Josephson dynamics.—In the presence of interactions between the atoms, $a_s \neq 0$, our system is well described by the nonlinear Gross-Pitaevskii equation (GPE) $i\hbar\dot{\Psi} = (H_0 + g_0 N|\Psi|^2)\Psi$, where $g_0 = 4\pi\hbar^2 a_s/m$ [27]. In the limit of an interwell barrier higher than the chemical potential—also identified as the tunneling regime—we can investigate the Josephson dynamics within a two-mode Josephson Gross-Pitaevskii (JGP) model. It consists, in analogy with the Rabi case, in writing the Gross-Pitaevskii wave function as a linear combination of two modes, $\psi_L^{\rm GP}$ and $\psi_R^{\rm GP}$. These modes are localized in the left and right well, respectively, and can be constructed with the sum and difference of the lowest energy symmetric and antisymmetric stationary states of the GPE, see [25]. The relative population $z(t)$ and phase $\phi(t)$ are conjugated dynamical variables whose evolution is provided by the "nonrigid pendulum" Josephson Hamiltonian [5]

$$H(z, \phi) = NU\frac{z^2}{2} - 2K\sqrt{1 - z^2}\cos\phi, \qquad (1)$$

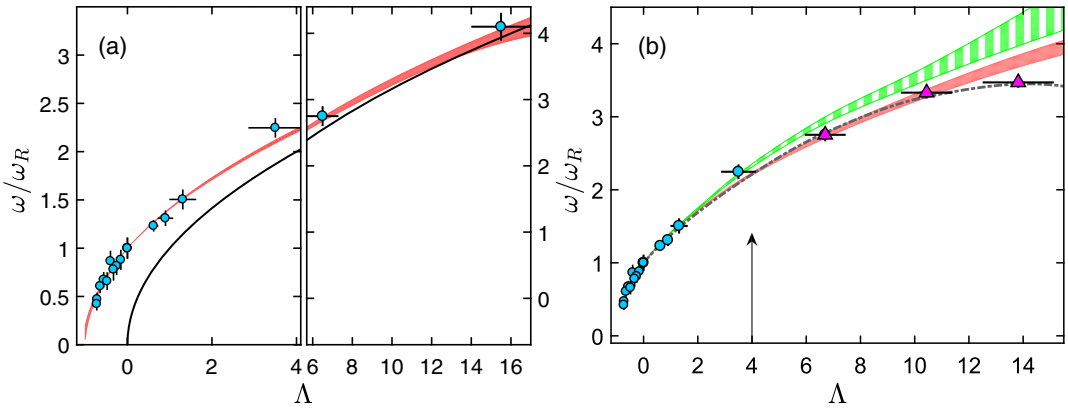

FIG. 2. Small amplitude oscillation frequency ω as a function of Λ (dots) crossing over attractive to repulsive interactions, $-1 \leq \Lambda \leq 16$. (a) Rabi to Josephson transition in the tunneling regime. The red solid area is the frequency ω_J calculated from the JGP model [see Eq. (2)]. The width of the area takes into account experimental fluctuations of the initial population imbalances z_0(0–0.2). The solid black line is the plasma frequency $\omega_p = \sqrt{2NKU}/\hbar$. (b) Additional measurements (see pink triangles) for $\Lambda > 4$ breaking the tunneling condition. The barrier height, set at small values of $\Lambda > 0$, is kept constant up to $\Lambda = 16$, while the scattering length is constantly increased. The arrow indicates the point where the chemical potential is equal to the barrier height. The red solid (green with stripes) area represents the JGP (TMS) model predictions. The dotted-dashed grey line interpolates the results of the GPE numerical analysis including the z_0 experimental values. The horizontal error bars of the data are due to the uncertainties in the atom numbers, scattering lengths, and trapping frequencies. See [25] for a detailed description of the experimental parameters.

with equation of motion $\dot{z}=dH(z,\phi)/d\phi$, $\dot{\phi}=-dH(z,\phi)/dz$, where $K = \int d^3\boldsymbol{r}\psi_R^{\mathrm{GP}} H_0 \psi_L^{\mathrm{GP}}$ and $U = g_0 \int d^3\boldsymbol{r}|\psi_{L,R}^{\mathrm{GP}}|^4$ is the interaction energy.

Equation (1) highlights the interplay between tunneling and interaction in the case of small-amplitude oscillations, that occur at frequency

$$\omega_J = \sqrt{4K^2 + 2NKU}/\hbar = 2K\sqrt{1+\Lambda}/\hbar, \qquad (2)$$

where $\Lambda = NU/2K$. A consequence of the nonrigidity of the pendulum described by Eq. (1) is to provide an ω_J that interpolates between the Rabi frequency $\omega_R = 2K/\hbar$ (for $NU \ll 2K$), and the Josephson "plasma" frequency $\omega_p = \sqrt{2NKU}/\hbar$ (for $NU \gg 2K$). Josephson plasma oscillations have been observed in superfluid and superconducting systems, while the transition from the Rabi to the Josephson regimes has remained elusive.

Following an experimental procedure similar to the one implemented in the noninteracting case, we record the oscillation frequency for BECs with different values of Λ ranging from $\Lambda = -1$ to 16. The results reported in Fig. 2(a) are obtained controlling both the scattering length over positive and negative values and the barrier height in order to remain in the tunneling regime. Experimental data (dots) are compared with the prediction of the JGP model, taking into account the initial value of the population imbalance. By tuning the scattering length to negative values, $\Lambda = (NU/2K) < 0$, we observe a slowing down of the oscillations with a divergence of the period for $\Lambda = -1$ in correspondence of the critical point of a quantum phase transition characterized by parity symmetry breaking [17,18]. By tuning the scattering length to positive values $\Lambda > 0$, we observe an increase of the plasma frequencies as predicted by theory. In particular, the experimental data clearly identify the "Rabi to Josephson" regime, Fig. 2(a), where Eq. (2) smoothly interpolates between Rabi and Josephson plasma oscillations. In Fig. 2(b), we intentionally exit the tunneling regime for $\Lambda > 4$ performing three additional measurements (see pink triangles) with increasing values of the scattering length while keeping the barrier height constant and equal to the values used for $\Lambda \gtrsim 0$. It is interesting to note that the agreement of the JGP model extends up to $\Lambda \simeq 10$, while for $\Lambda > 10$, only a full numerical solution of the GPE can recover the agreement with the experimental data.

We remark here that, in the range $-1 < \Lambda < 1$, the experimental frequencies are well described with the coupling and interaction terms of Eq. (1) calculated with the wave functions $\psi_{L,R}$ of the noninteracting Schrödinger equation, see [25]. In the following, we will refer to this model as the two-mode Schrödinger (TMS) model. This is a good approximation whenever $|a_s|N/a_{\mathrm{ho}} \ll 1$ (with a_{ho} being the harmonic oscillator (ho) length of the single well trap) so that the interaction is small enough to provide a perturbative correction [see Fig. 2(b)]. In this regime, the Josephson Hamiltonian can be mapped to a system of N bosons governed by the Lipkin-Meshov-Glick Hamiltonian [28] and spanning the symmetrized subsection of the full Hilbert space. This regime has been realized, so far, only with spinor BECs and has been exploited for the creation of atomic quantum entangled states [24,29]. However, the amount of entanglement has been limited, so far, mainly by inelastic collisions that lead to two- and three-body losses. We expect that such limits will be overcome in our system

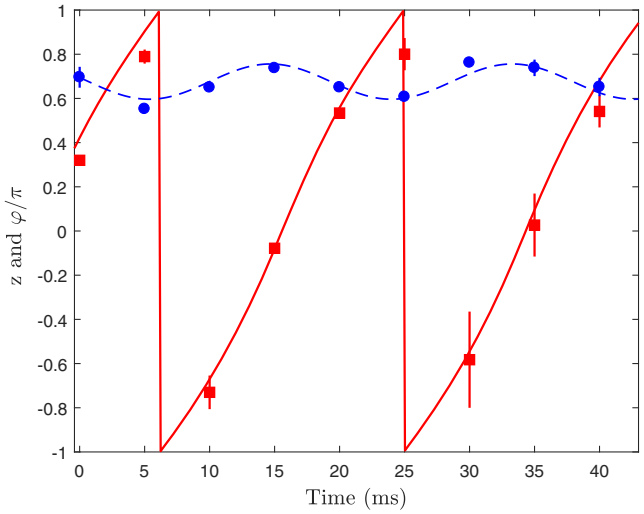

FIG. 3. Macroscopic quantum self-trapping. Time evolution of the population imbalance (blue points) and relative phase (red squares) for the MQST dynamics, for $2K/h = 5$ Hz and $\Lambda \sim 10$. The blue dashed line is a sinusoidal fit to the data. The red line is the theoretical prediction, see [25].

where two-body inelastic losses are forbidden by energy and angular momentum conservations (the atoms are in the absolute internal ground state) and three body inelastic losses are suppressed by the use of a broad magnetic Feshbach resonance.

Macroscopic quantum self-trapping.—In contrast to the noninteracting case (see Fig. 1), the oscillation frequency, in the presence of interactions, depends on the initial value of the population imbalance z_0. When $|z_0|$ becomes larger than a critical imbalance [25],

$$z_c = \frac{2}{NU}\sqrt{2KNU - 4K^2}, \tag{3}$$

the initial interaction energy $NUz_0^2/2$ becomes larger than the tunneling energy $2K$ in Eq. (1) and the system cannot reach the balanced $z = 0$ configuration due to energy conservation. In the MQST regime, the population imbalance oscillates around a nonzero average value $\langle z(t)\rangle \neq 0$ and a running-phase condition is established. For evolution times that are not too long, we observe coherent, undamped, oscillations in the population and phase (on top of a steadily increasing value), see Fig. 3. At longer times, dephasing and decoherence are expected to slow down the oscillations and eventually break down the MQST [30].

We have explored the occurrence of MQST by studying the frequency oscillations as a function of the population imbalance z_0 and unveiling the slowing of the dynamics in correspondence with the critical imbalance z_c (see Fig. 4). We have chosen three different experimental configurations [Figs. 4(a)–4(c)] for different interaction strengths and tunneling, but with a fixed critical imbalance $z_c \approx 0.5$. For high barriers, in the tunneling regime, see Fig. 4(a), we found a good agreement between the experimental results and the theoretical predictions of the JGP model, according to Eq. (3). In Fig. 4(b), the barrier height is smaller than the chemical potential, and the JGP model fails to describe the experimental results correctly. The agreement can be recovered from a full two-mode expansion of the nonlinear term of GPE, which we call the two-mode Gross-Pitaevskii model (TMGP) [7,31]. We can show that JGP is in agreement with the TMGP after renormalizing the coupling term K to $K - NI_3$ [25] where $I_3 = g_0 \int d\boldsymbol{r}\psi_R^{\mathrm{GP}}(\psi_L^{\mathrm{GP}})^3 = g_0 \int d\boldsymbol{r}\psi_L^{\mathrm{GP}}(\psi_R^{\mathrm{GP}})^3$. Finally, for even lower barriers, the two-mode Gross-Pitaevskii approximations fail in the description of the experimental results, and a full numerical solution of the GPE is necessary. It is interesting to notice that a self-trapping phenomenon still persists not only beyond the Josephson tunneling regime,

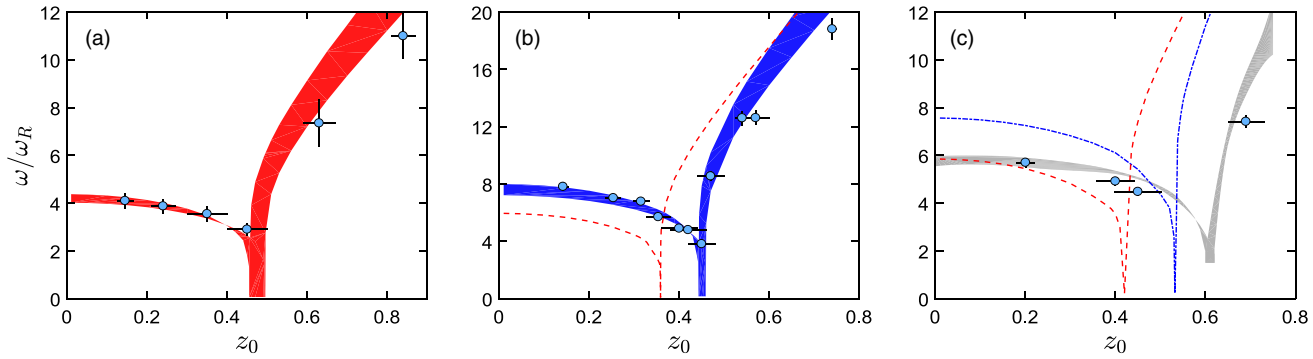

FIG. 4. Oscillation frequency as a function of the maximum atomic imbalance z_0 for (a) $2K/h = 4.3$ Hz, $a_s = 1\,a_0$, $\Lambda = 17$ (b) $2K/h = 6.7$ Hz, $a_s = 4\,a_0$, $\Lambda = 30$, and (c) $2K/h = 16$ Hz, $a_s = 12\,a_0$, $\Lambda = 20$. The total atom number is $N = 7000 \pm 300$ and approximately constant for the three sets of measurements. The values of the chemical potential and the interwell barrier are (a) $\mu/h = 410$ Hz, $V_0 = h \times 540$ Hz; (b) $\mu/h = 480$ Hz, $V_0 = h \times 475$ Hz; (c) $\mu/h = 530$ Hz, $V_0 = h \times 355$ Hz. The red solid area in panel (a) and red dashed lines in (b) and (c) are the theoretical predictions of the JGP model. The blue solid area in (b) and dashed-dotted line in (c) are the theoretical predictions of the TMGP model. The gray solid area in (c) is the result of numerical integration of the GPE.

but even with the height of the barriers much smaller than the chemical potential when the two-mode ansatz breaks down. In these cases, however, the self-trapping is not accompanied by coherent population-phase oscillations, but it is expected to decay though the creation of topological excitations [12]. The self-trapped regime was first demonstrated in [9] and coherent population in the ac-Josephson regime, where an average population imbalance was induced by an external drive, was observed in [13].

Conclusions.—We have reported the detailed characterization of the competition between tunneling and interactions in the dynamics of a bosonic Josephson junction made of ultracold atoms in regimes not accessible with different superfluid or superconducting systems. The Rabi oscillations of noninteracting BECs provide the first demonstration of a linear two-mode beam splitter for a trapped condensate in a double-well potential and open important perspectives in the field of atomtronics [32] and quantum metrology thanks to the possibility of performing both linear and nonlinear operations between the two modes on demand [24]. Our experiment opens the possibility of studying the quantum dephasing of Josephson dynamics [33], quantum fluctuations of work in a mesoscopic quantum system [34], and coherent Shapiro steps up to the onset of quantum chaos and turbulence by modulating, in time, the height of the tunneling barrier and/or the trapping frequencies, also in concomitance with the creation of topological defects [35]. Further many-body dynamical effects include the collapse and revival of the coherence [36] and the creation of quantum entanglement [21–24].

We thank all our colleagues of the Quantum Degenerate Gases group at LENS for inspiring discussions. This work was supported by the ERC Starting Grant AISENS No. 258325 and by EC-H2020 Grant QUIC No. 641122.

[1] A. Barone and G. Paternò, *Physics and Applications of the Josephson Effect* (John Wiley & Sons, New York, 1982).
[2] K. K. Likharev, Rev. Mod. Phys. **51**, 101 (1979).
[3] S. V. Pereverzev, A Loshak, S. Backhaus, J. C. Davis, and R. E. Packard, Nature (London) **388**, 451 (1997); J. C. Davis and R. E. Packard, Rev. Mod. Phys. **74**, 741 (2002).
[4] O. Avenel and E. Varoquaux, Phys. Rev. Lett. **55**, 2704 (1985).
[5] A. Smerzi, S. Fantoni, S. Giovanazzi, and S. R. Shenoy, Phys. Rev. Lett. **79**, 4950 (1997); S. Raghavan, A. Smerzi, S. Fantoni, and S. R. Shenoy, Phys. Rev. A **59**, 620 (1999).
[6] I. Zapata, F. Sols, and A. J. Leggett, Phys. Rev. A **57**, R28 (R) (1998); A. Smerzi and A. Trombettoni, Phys. Rev. A **68**, 023613 (2003); B. Julia-Diaz, A. D. Gottlieb, J. Martorell, and A. Polls, Phys. Rev. A **88**, 033601 (2013); M. Abad, M. Guilleumas, R. Mayol, F. Piazza, D. M. Jezek, and A. Smerzi, Europhys. Lett. **109**, 40005 (2015); A. Burchianti, C. Fort, and M. Modugno, Phys. Rev. A **95**, 023627 (2017).
[7] D. Ananikian and T. Bergeman, Phys. Rev. A **73**, 013604 (2006).
[8] F. S. Cataliotti *et al.*, Science **293**, 843 (2001).
[9] M. Albiez, R. Gati, J. Fölling, S. Hunsmann, M. Cristiani, and M. K. Oberthaler, Phys. Rev. Lett. **95**, 010402 (2005).
[10] T. Schumm, S. Hofferberth, L. M. Andersson, S. Wildermuth, S. Groth, I. Bar-Joseph, J. Schmiedmayer, and P. Krüger, Nat. Phys. **1**, 57 (2005).
[11] L. J. LeBlanc, A. B. Bardon, J. McKeever, M. H. T. Extavour, D. Jervis, J. H. Thywissen, F. Piazza, and A. Smerzi, Phys. Rev. Lett. **106**, 025302 (2011).
[12] G. Valtolina *et al.*, Science **350**, 1505 (2015).
[13] S. Levy, E. Lahoud, I. Shomroni, and J. Steinhauer, Nature (London) **449**, 579 (2007).
[14] K. G. Lagoudakis, B. Pietka, M. Wouters, R. André, and B. Deveaud-Plédran, Phys. Rev. Lett. **105**, 120403 (2010).
[15] M. Abbarchi *et al.*, Nat. Phys. **9**, 275 (2013).
[16] C. Chin, R. Grimm, P. Julienne, and E. Tiesinga, Rev. Mod. Phys. **82**, 1225 (2010).
[17] A. Trenkwalder *et al.*, Nat. Phys. **12**, 826 (2016).
[18] J. I. Cirac, M. Lewenstein, K. Molmer, and P. Zoller, Phys. Rev. A **57**, 1208 (1998).
[19] M. J. Steel and M. J. Collett, Phys. Rev. A **57**, 2920 (1998).
[20] D. R. Dounas-Frazer, A. M. Hermundstad, and L. D. Carr, Phys. Rev. Lett. **99**, 200402 (2007); L. D. Carr, D. R. Dounas-Frazer, and M. A. Garcia-March, Europhys. Lett. **90**, 10005 (2010).
[21] T. Barrada, S. van Frank, R. Bücker, T. Schumm, J.-F. Schaff, and J. Schmiedmayer, Nat. Commun. **4**, 2077 (2013).
[22] L. Pezzè, L. A. Collins, A. Smerzi, G. P. Berman, and A. R. Bishop, Phys. Rev. A **72**, 043612 (2005).
[23] J. Estève, C. Gross, A. Weller, S. Giovanazzi, and M. K. Oberthaler, Nature (London) **455**, 1216 (2008).
[24] L. Pezzè, A. Smerzi, M. Oberthaler, R. Schmidt, and P. Treutlein, arXiv:01609.1609.
[25] See Supplemental Material at http://link.aps.org/supplemental/10.1103/PhysRevLett.118.230403 for details on the experimental configuration and phase readout, a description of the experimental parameters of the Rabi and small-amplitude plasma oscillations, and further discussions on the two-mode Gross-Pitaevskii model.
[26] C. D'Errico, M. Zaccanti, M. Fattori, G. Roati, M. Inguscio, G. Modugno, and A. Simoni, New J. Phys. **9**, 223 (2007).
[27] F. Dalfovo, S. Giorgini, L. P. Pitaevskii, and S. Stringari, Rev. Mod. Phys. **71**, 463 (1999).
[28] H. J. Lipkin, N. Meshkov, and A. J. Glick, Nucl. Phys. **62**, 188 (1965); V. V. Ulyanov and O. B. Zaslavskii, Phys. Rep. **216**, 179 (1992).
[29] C. Gross, T. Zibold, E. Nicklas, J. Estève, and M. K. Oberthaler, Nature (London) **464**, 1165 (2010); M. F. Riedl, P. Böhi, Y. Li, T. W. Hänsch, A. Sinatra, and P. Treutlein, Nature (London) **464**, 1170 (2010); H. Strobel, W. Muessel, D. Linnemann, T. Zibold, D. B. Hume, L. Pezzè, A. Smerzi, and M. K. Oberthaler, Science **345**, 424 (2014).
[30] J. Ruostekoski and D. F. Walls, Phys. Rev. A **58**, R50 (1998).
[31] S. Giovanazzi, A. Smerzi, and S. Fantoni, Phys. Rev. Lett. **84**, 4521 (2000).
[32] S. Eckel, J. G. Lee, F. Jendrzejewski, N. Murray, C. W. Clark, C. J. Lobb, W. D. Phillips, M. Edwards, and G. K.

Campbell, Nature (London) **506**, 200 (2014); R. A. Pepino, J. Cooper, D. Z. Anderson, and M. J. Holland, Phys. Rev. Lett. **103**, 140405 (2009); D. Aghamalyan, M. Cominotti, M. Rizzi, D. Rossini, F. Hekking, A. Minguzzi, L.-C. Kwek, and L. Amico, New J. Phys. **17**, 045023 (2015).

[33] A. Vardi and J. R. Anglin, Phys. Rev. Lett. **86**, 568 (2001).

[34] R. G. Lena, G. M. Palma, and G. De Chiara, Phys. Rev. A **93**, 053618 (2016).

[35] F. Piazza, L. A. Collins, and A. Smerzi, New J. Phys. **13**, 043008 (2011); C. Lee, Phys. Rev. Lett. **102**, 070401 (2009).

[36] G. J. Milburn, J. Corney, E. M. Wright, and D. F. Walls, Phys. Rev. A **55**, 4318 (1997).